



ELSEVIER

Journal of Biochemical and Biophysical Methods
1553 (2002) xxx–xxx

JOURNAL OF
biochemical and
biophysical
methods

www.elsevier.com/locate/jbbm

Novel methodology for the follow-up of acute lymphoblastic leukemia using FTIR microspectroscopy

J. Ramesh^a, J. Kapelushnik^b, J. Mordechai^c, A. Moser^b,
M. Huleihel^d, V. Erukhimovitch^d, C. Levi^a, S. Mordechai^{a,*}

^aDepartment of Physics, Ben Gurion University, Beersheba, 84105, Israel

^bPediatric Hematology-Oncology, Soroka University Medical Center, Beersheba, 84105, Israel

^cDepartment of Pediatric Surgery, Soroka University Medical Center, Beersheba, 84105, Israel

^dInstitute of Applied Sciences, Ben Gurion University, Beersheba, 84105, Israel

Received 21 August 2001; received in revised form 19 November 2001; accepted 14 December 2001

Abstract

In this report, we present a novel spectroscopic method of follow-up during chemotherapy treatment for B- and T-cell childhood leukemia patients. We isolated peripheral lymphocytes from blood drawn from patients before and after the chemotherapy and collected Microscopic FTIR (FTIR-MC) spectra of the isolated lymphocytes. Our results showed that nucleic acids content decreased in both types of patients. Changes in phospholipids and proteins level could be observed. The overall effects of drugs administered to the patients can be understood at the molecular level using FTIR-MC and these results are expected to stimulate wider applications of spectroscopy in leukemia research. © 2002 Elsevier Science B.V. All rights reserved.

Keywords: Acute lymphoblastic leukemia; Drugs; Follow-up; Lymphocytes; FTIR microspectroscopy

1. Introduction

Leukemia accounts for one-third of all childhood cancers in children. Acute lymphoblastic leukemia (ALL) is a predominant type of childhood leukemia with varying incidence in different countries ranging from 0.9 to 4.7 per 100,000 children [1]. Radiation, environmental agents, maternal alcohol consumption and paternal smoking are associated

* Corresponding author. Tel.: +972-8-646-1749; fax: +972-8-647-2903.

E-mail address: shaulm@bgumail.bgu.ac.il (S. Mordechai).

with increased risk of ALL in children [2]. ALL is a clonal hematological disorder arising due to genetic changes in hemopoietic cells [3]. The genetic alterations in transcription factor oncogenes are mainly implicated in the process of leukemogenesis [4]. Treatment of ALL using combination therapy has drastically improved the survival rate in the case of children [5]. In the clinics, to detect the minimal residual disease, highly sensitive PCR techniques are applied [6].

Since the last decade, FTIR has proven to be a powerful tool in medicine. Objective diagnosis is becoming a reality with the advanced microscopic FTIR (FTIR-MC) spectroscopy [7,8]. Literature has many examples for early diagnosis of malignancy using FTIR-MC. Gao et al. [9] has carried out FTIR study of human breast, normal and carcinomal tissues. They reported that their method of analysis results in nearly 100% diagnostic accuracy of carcinomal tissues from normal ones. The chronic lymphocytic leukemia could be well characterized by FTIR based on lipid and DNA content and the overall spectral characters [10]. Our group has successfully applied FTIR-MC in the characterization of cells [11,12] and optical diagnosis of colon cancer [13]. This report presents the application of FTIR-MC in the follow-up of chemotherapy treatment of two children who had B- and T-cell type ALL. This is the first report of this kind showing the potential of FTIR-MC for the follow-up of leukemia chemotherapy treatment in children.

2. Materials and methods

2.1. Clinical procedures

The physicians in the department of Pediatric Hematology-Oncology at the Soroka University Medical Center (SUMC) provided the blood samples from two children who had B- and T-cell ALL. Two children, aged 4 and 15 years old, were admitted to SUMC in December 2000 and January 2001, respectively. The blasts are malignant B or T cells present in the peripheral lymphocytes isolated from the patient. Their percentage of blasts was 85 and 68 at the time of admission for B- and T-cell ALL patients, respectively. Standard chemotherapy treatment protocol (BFM 95) was followed for both patients. The blood was processed immediately for the isolation of the lymphocytes. Lymphocytes were isolated as previously described [14]. Briefly, 3 ml of blood were loaded over 3 ml of Histopaque (purchased from Sigma USA) solution and centrifuged at $300 \times g$ for 30 min at 23°C . The Histopaque solution is the mixture of Metrizoic acid and Ficoll solution having density of 1.077 g/ml. The lymphocyte layer (mononuclear cells), located at the middle of the tube, was isolated. The separated lymphocytes were washed again with 10 ml of PBS by centrifugation at $300 \times g$ for 10 min at 23°C . The sample was checked for the red blood cells (RBC) contamination. This procedure ensures high quality lymphocytes. Blast count was performed using normal optical microscope inspection and flow cytometry techniques.

2.2. FTIR microspectroscopy

FTIR-measurements were performed in transmission mode using the FTIR microscope IRscope II with sensitive MCT detector, which is coupled to the FTIR spectrometer

(BRUKER EQUINOX model 55/S OPUS software). The microscope is also equipped with a CCD-camera for the visible range of the spectrum, and a fully computerized X – Y stage, which allows measurement of large number of spectra that can be used for creating FTIR chemical-maps. The isolated lymphocytes were loaded (about 100 cells per 50- μ m diameter) on Zinc–Selenium (ZnSe) crystals and later dried completely. The measured spectra cover the wave number range 600–4000 cm^{-1} . In the case of patients, the spectra were recorded before and during the chemotherapy treatment. During each measurement, the measured sites were circular of about 50- μ m diameter at most. Such area contains enough lymphocytes to obtain good quality spectra with high signal-to-noise ratio. The spectra taken were average of 128/256 scans to increase the signal-to-noise ratio. The baseline was corrected as follows. Initially, the spectrum was divided into 64 sections of equal size. Then the y -value minima of the spectrum were connected, generating a curve which gives the best fit to the background. Amide I normalization was performed for all the spectra to take care of the variations in the total number of mononuclear cells (lymphocytes) sampled in every measurement. For each sample, the spectrum was taken as the average of 10 different measurements. The signal-to-noise ratio was calculated for all the measurements and only spectra with high signal-to-noise ratio (≥ 1000) were used for further data analysis. Integrated absorbance was calculated using ORIGIN software and the error bars represent the maximum S.D. obtained in all of our measurements.

3. Results

3.1. B-cell ALL patient

Microscopic FTIR spectra of lymphocytes isolated from the blood of two children having B- and T-cell ALL, respectively are shown in Fig. 1a and b. In both spectra, A is the average of four age-matched healthy controls. No major spectral changes were observed between the average of four controls (Fig. 1a: A) and the spectra of patients before the beginning of treatment (Fig. 1a: B). But there were minor changes in the absorbance of symmetric (1000–1100) and asymmetric (1200–1245) regions of the phosphate group and also in the amide II region arising from the proteins. For clarity reasons, only the spectra obtained after (C) 15 and (D) 30 days of treatment were presented. The spectra (Fig. 1a: C) and (Fig. 1a: D) clearly showed decrease in the absorbance of phosphate bands corresponding to nucleic acids. Also the band at 965 cm^{-1} accounting for the symmetric stretching vibration of the phosphodiester bonds in nucleic acids showed reduction in the intensity before and after the treatment. The standard deviation (S.D.) divided by the square root of number of measurements for the complete region (800–3200 cm^{-1}) is shown in Fig. 1a and b. Our S.D. analysis showed that the difference between the sample before treatment and last (22/30) day of treatment was large and it was found to be in the symmetric and asymmetric stretching vibration of phosphate containing metabolites. The error bars in Figs. 2–4 were calculated from the values of the standard deviation.

In addition, spectral pattern changes were observed for the phosphate bands. No significant changes in the amide II band were observed. Fig. 1b shows the microscopic FTIR spectra of controls, before treatment and during the chemotherapy treatment of the

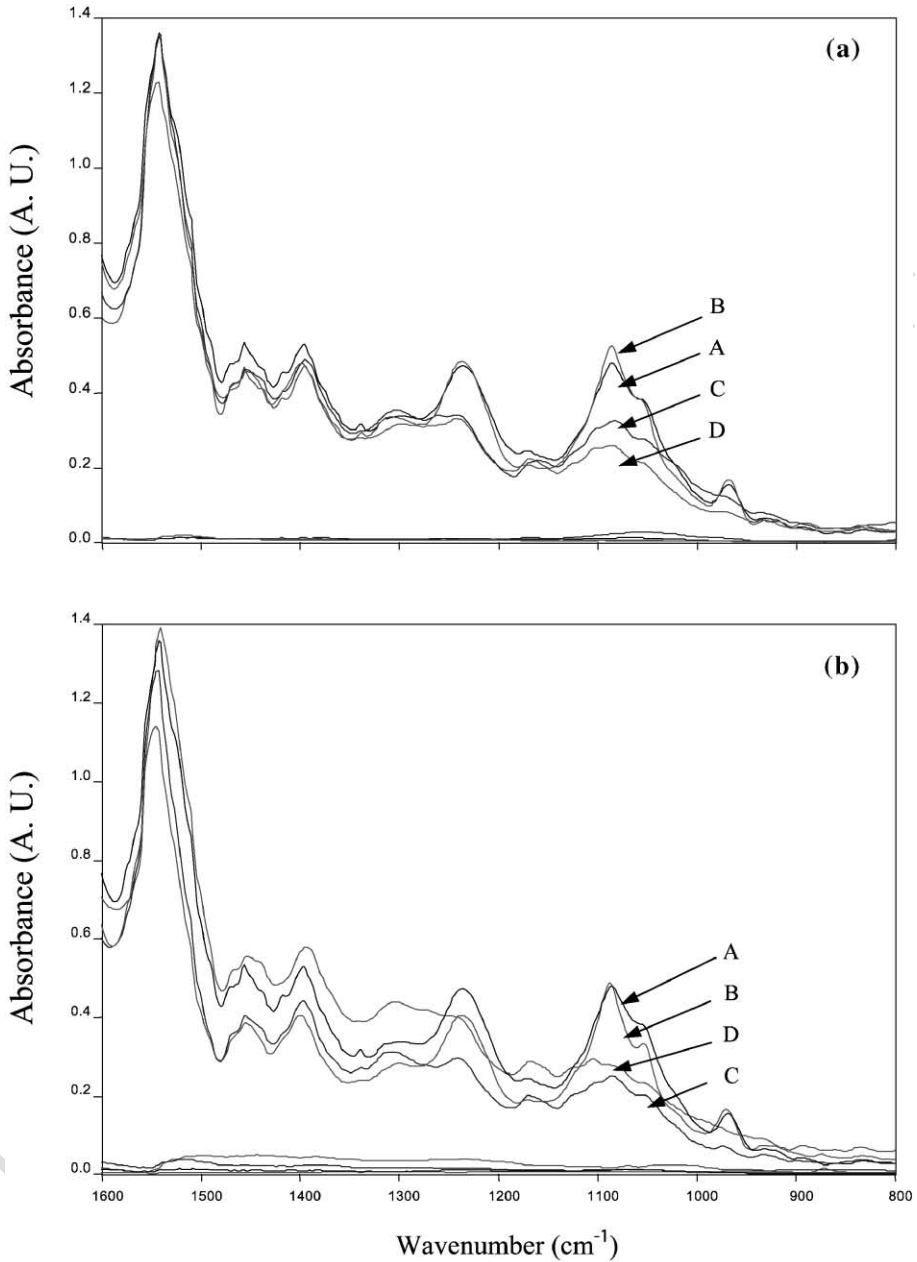


Fig. 1. (a) FTIR microspectroscopy of lymphocytes isolated from a B-cell ALL patient. A: Controls, B: before treatment, C: 15 days of treatment, D: 30 days of treatment. Amide I normalization has been applied to all the spectra. (b) FTIR microspectroscopy of lymphocytes isolated from T cell ALL patient. A: average of four controls, B: day 0 (before the treatment), C: day 11 after treatment, D: day 22 after treatment. The lines at the bottom of the spectra represent the standard deviations divided by the square root of the number of measurements.

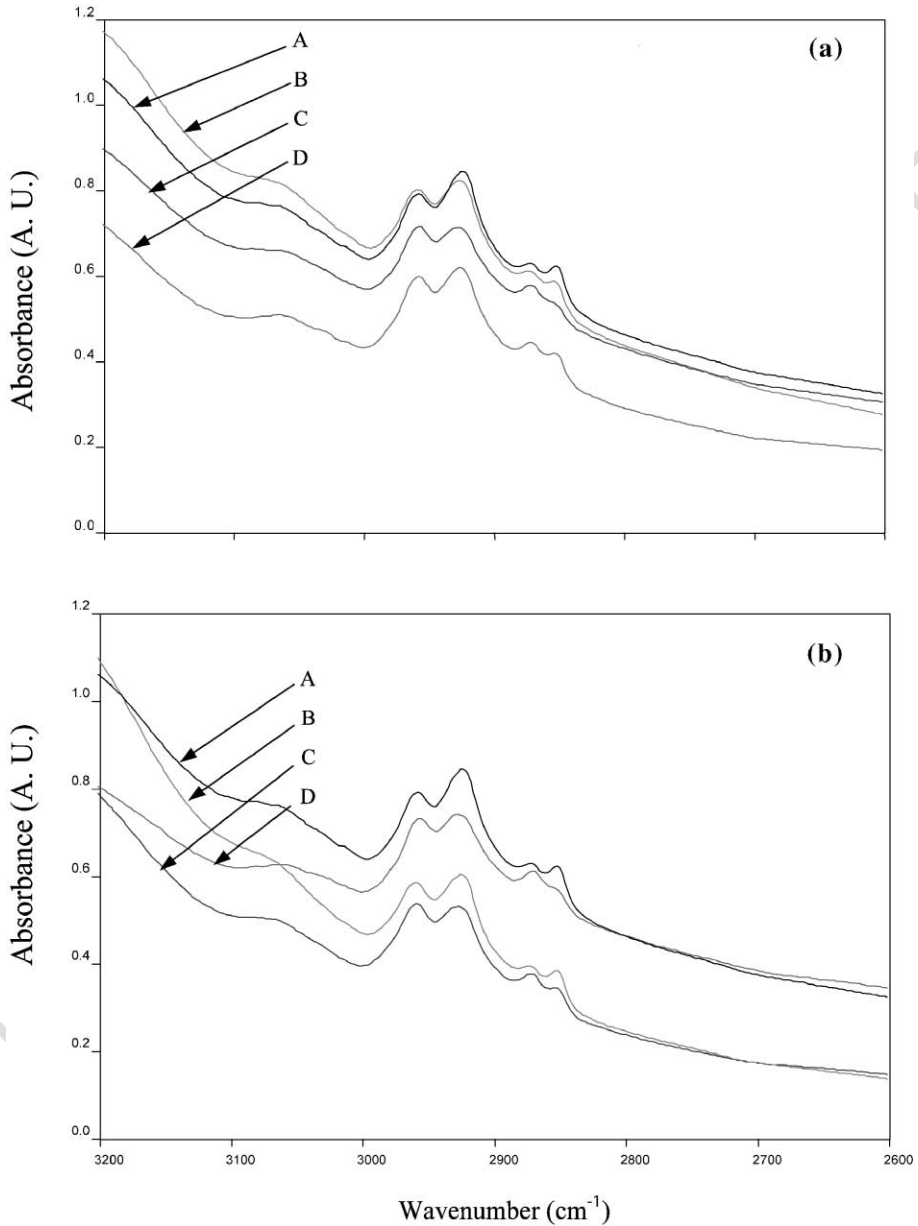


Fig. 2. (a) FTIR microspectroscopy of lymphocytes from a B-cell ALL patient. The labels are the same as in Fig. 1. (b) FTIR microspectroscopy of lymphocytes from a T-cell ALL patient. The samples are the same as in Fig. 1.

T-cell ALL patient. The chemotherapy treatment caused drastic molecular changes in the cells, which could be observed in the spectra for the B-cell ALL patient.

Figs. 2a shows FTIR-MC spectra in the region $2600\text{--}3200\text{ cm}^{-1}$ for B-cell ALL patient. There was no change in the absorbance between the controls and the sample taken before the treatment. As the treatment proceeded, the absorbance decreased in a systematic manner for 15 and 30 days of treatment.

The variation of phosphate levels was measured by integrating the absorbance between symmetric ($1000\text{--}1150\text{ cm}^{-1}$) and asymmetric ($1170\text{--}1310\text{ cm}^{-1}$) bands is presented in Figs. 3a. The total phosphate content declined sharply on the 7th day of treatment and gradually increased till the 12th day. Later it was observed to decrease steadily from 12 to 23 days of treatment.

The region between 2800 and 3000 cm^{-1} accounts for symmetric and asymmetric stretching vibrations of CH_2 and CH_3 groups from proteins, nucleic acids and phospho-

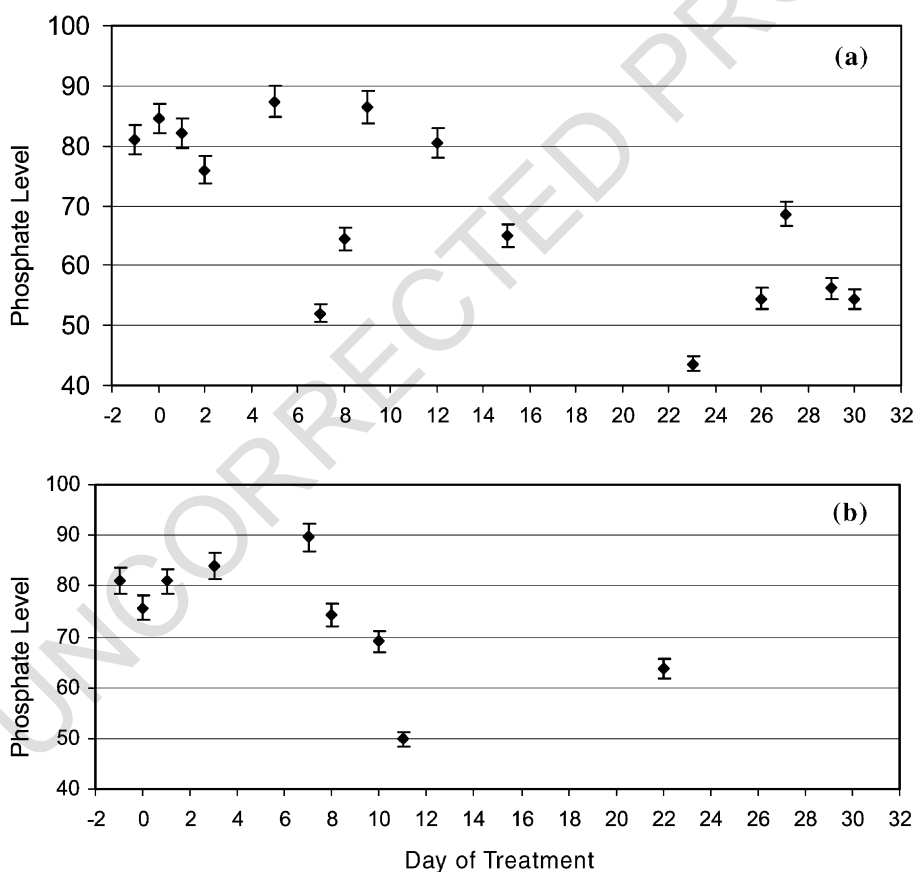


Fig. 3. Phosphate content is presented as the integrated absorbance comprising symmetric and asymmetric stretching vibrations of phosphate group in the nucleic acids. (a) B-cell ALL patients, (b) T-cell ALL patients. Day 1 is the average of four controls and day 0 stands for the day before treatment.

lipids [15] in the cells. Integrated absorbance (IA) covering this region for B-cell ALL patient is shown in Fig. 4a. Controls and the patient before treatment had the same value and a steady decrease was observed after beginning of the treatment. There were fluctuations during the course of 30 days. Linear square fit for 12 data points covering 30 days of treatment is shown in Fig. 4a. The deduced slope (-0.90 ± 0.19) indicates that there were overall tendencies of decrease in the IA for the B-cell ALL patient. Table 1 shows the percentage of blasts and the results showed that the blast percentage drastically decreased with chemotherapy treatment, which was reflected in the contents of cell metabolites.

3.2. T-cell ALL patient

Similar to B-cell ALL case, the spectra of lymphocytes isolated from T-cell ALL patient before treatment (Fig. 1b: B) did not show absorbance changes in the phosphate region in comparison to the controls (Fig. 1b: A). However, in the region between 1400

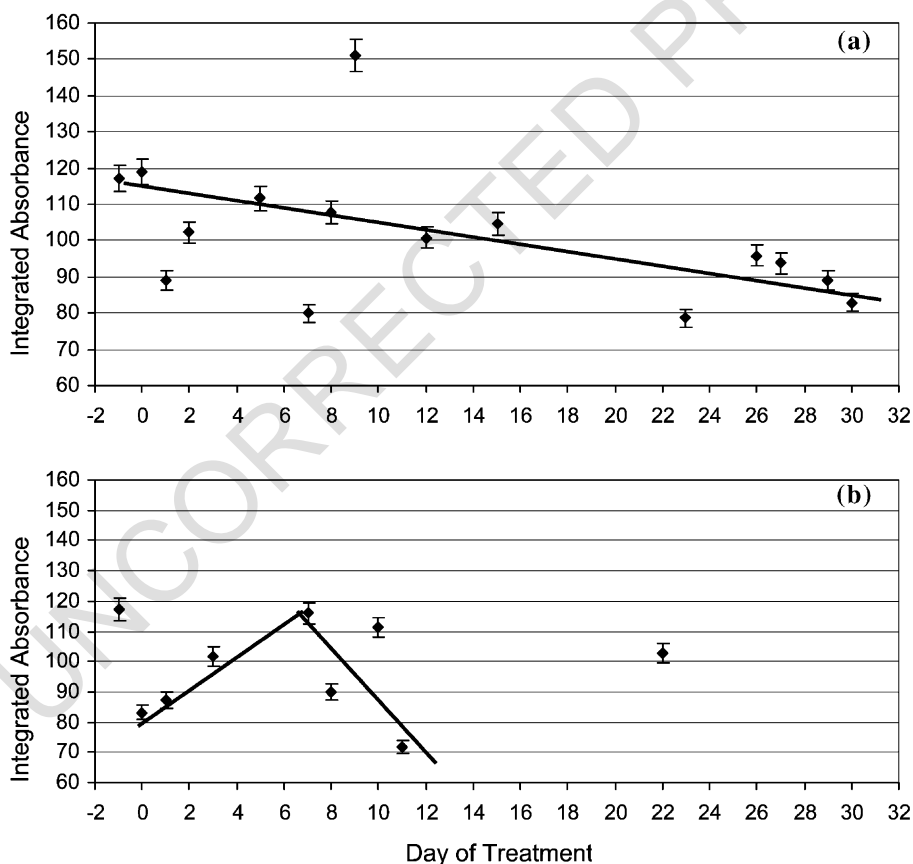


Fig. 4. Integrated absorbance between 2800 and 3000 cm^{-1} for (a) B-cell ALL patients, (b) T-cell ALL patients. Day of treatment labels are the same as in Fig. 3. The lines represent linear square fits to the data.

t1.1 Table 1

t1.2 The percentage of blasts from the day of admission to the medical center

t1.3	Day of treatment	B-cell ALL	T-cell ALL
t1.4	0	85	68
t1.5	1	65	–
t1.6	3	–	1
t1.7	4	42	–
t1.8	5	–	1
t1.9	7	2	–

and 1600 cm^{-1} , there were notable changes in the intensity between the controls and the sample before treatment. Decrease in protein concentration was evident with lower intensity for the amide II band. During the chemotherapy treatment, significant changes in the spectra were observed. The spectra measured on the 11th day of treatment showed sudden decrease in the absorbance in the entire region ($900\text{--}1800\text{ cm}^{-1}$). In addition, broadening of the peaks was observed in the phosphate region. The spectra collected on the 22nd day of treatment also showed dramatically lower phosphate content with much lower absorbance in the region between 1000 and 1200 cm^{-1} compared to the spectrum before treatment (day 0). The changes were specific in biomolecular composition, as the spectral crossover could be observed from 1300 to 1600 cm^{-1} .

The spectra in the region between 2600 and 3200 cm^{-1} for the T-cell ALL patient are shown in Fig. 2b. In this case, the absorbance was higher for controls than the sample collected before the chemotherapy treatment. After 11 days of treatment, the decrease in absorbance continued and began to return to the controls level after 22 days of treatment.

Total phosphate level shown in Fig. 3b for T-cell ALL patient decreased from the 8th day of treatment and reached a saturation on the 22nd day of treatment. The rate of decrease in this case was high in comparison to B-cell ALL.

Integrated absorbance calculated for the region between 2800 and 3000 cm^{-1} for T-cell ALL is presented in Fig. 4b. Interestingly, in the case of T-cell ALL patient, the IA for patient was lower by 50% compared to the controls. In addition, the chemotherapy treatment increased the IA steadily and reached the saturation on 10th day. We also observed fluctuations between 6 and 12 days. Least square fit analysis indicated that there were probably two slopes reflecting an increased absorbance ($+4.76\pm 0.54$) for 0–6 days followed by a local decrease (-6.67 ± 6.31) for 7–11 days of the treatment. Our results on the number of blasts indicated that both patients had high percentage of blasts. Blasts percentage was higher for B-cell ALL patient than the T cell patient and both patients responded well to the therapy showing dramatic reduction in the total percentage of blasts after few days of treatment. The percentage of blasts in the case of T-cell ALL is presented in Table 1. As in the B cell case, the blast percentage significantly decreased due to chemotherapy and the subsequent changes in the spectra were also observed.

4. Discussion

ALL is a major leukemia type among children and extensive research till today has achieved remarkable progress in the areas of treatment and follow-up during the course of

the treatment. Our studies gain special significance giving the nature that biomolecular changes occur upon the action of various drugs during therapy using an advanced optical technique. Earlier reports showed that in the case of chronic lymphoblastic leukemia (CLL) in adults, the FTIR spectra could be used to distinguish normal cases from patients [16]. In our study, only T-cell ALL could be differentiated from the controls by means of absorbance changes in the 1300–1600 cm^{-1} which include substantial decrease in the protein content for patients. Predominant spectral changes occurred in the region between 1000 and 1200 cm^{-1} which correspond to the nucleic acids in the cells. This observation is in agreement with the marked reduction in the percentage of blasts in both B and T cell patients due to chemotherapy treatment. It is important to note that the spectra after a week of chemotherapy treatment correspond to the normal population of the lymphocytes with drastic reduction in the percentage of blasts. Also, results obtained in this study give the picture of dynamic equilibrium of lymphocytes present in the blood samples of the patients. On the administration of chemotherapy drugs into a leukemia patient, the blasts (cancerous B or T cells) are killed but are still present in the circulating blood. It should be kept in mind that after a week of chemotherapy, the blast count gets reduced dramatically. These drugs act also on normal lymphocytes present in the blood. The equilibrium population of lymphocytes accounts for the lymphocytes (normal and blasts) affected by the drugs and newborn lymphocytes which are produced by the bone marrow. Within the duration of action of the chemotherapy drugs, the blood drawn by the physician contains the lymphocytes acted by drugs and also the unaffected lymphocytes circulating in the blood. However, FTIR-MC was sensitive to biomolecular changes in mononuclear cells upon the action of drugs.

The higher wave number region between 2800 and 3000 cm^{-1} give interesting clues to biomolecular changes due to chemotherapy. In the case of B-cell ALL, the decrease in IA during chemotherapy may be due to dramatic reduction in the nucleic acids or phospholipids. Absence of absorbance changes in the amide II rules out the major change in protein content in the cells. In the case of T-cell ALL, decrease in the IA for the sample before treatment may be due to the decreased protein or phospholipids content. This conclusion is supported by the decrease in absorbance in the amide II band for the sample before treatment in comparison to the controls whereas the protein content remained constant during the chemotherapy treatment. In view of monitoring the therapy, the increasing trend in the IA after 22 days of treatment can be considered as a progress, as it approaches the controls.

Anti-leukemia drugs administered for leukemia patients are known to inhibit the synthesis of nucleic acids. In particular, the effects of Methotrexate (MTX), L-Asparaginase and Doxorubicin are well-documented in the literature [17]. In particular, MTX is a structural analog of folic acid required for synthesis of bases in the nucleic acids. It inhibits the enzyme dihydrofolate reductase (DHFR) responsible for synthesis of precursors of nucleic acids. Doxorubicin which belongs to antitumor antibiotics class, acts as interchelator of DNA, thereby inhibiting the nucleic acids production in the tumor cells. Inhibition of nucleic acids synthesis leads to arresting the proliferation of blasts in the leukemia patients. In our study, we observed the decrease in DNA and RNA immediately after the beginning of the chemotherapy treatment with MTX for both patients. The reduction in DNA content was confirmed by the decrease in total phosphate content. This

was confirmed by two different methods of analysis of the FTIR spectra such as, 217
 integrating the absorbance comprising the symmetric and asymmetric stretching bands 218
 and also the ratio of integrated area of amide I/II regions (data not shown). In addition, the 219
 spectra showed significant decrease in absorption at 965 and 1245 cm^{-1} arising from 220
 phosphodiester bonds in the nucleic acids (data not shown). The difference in the rate of 221
 decrease between B and T-cell ALL patients are not clearly understood. Discrete 222
 fluctuations observed for B-cell ALL patient may be due to the variations in the immune 223
 system. 224

This report gives glimpse of the application of modern FTIR techniques in leukemia 225
 research. We showed that FTIR-MC could be used to understand the molecular changes in 226
 the cells following chemotherapy treatment. The advantages of this method are fast, 227
 economical and objective. Efforts are in progress in our lab to correlate the vast amount of 228
 clinical information existing on these two patients with FTIR-MC studies. Our studies will 229
 pave the road to online monitoring of patients during chemotherapy using advanced 230
 optical techniques, which can be foreseen in the future. 231

Acknowledgements 232

We gratefully acknowledge the Harry Stern Applied Research Fund, Prof. Y. Tabb 233
 Research Fund for Cancer Research and the Israel Science Foundation (ISF grant number: 234
 788/01) for financial support. We also thank Mrs. Marina Talyshinsky for technical support 235
 during this work. 236

References 237

- [1] Ma SK, Wan TSK, Chan LC. Cytogenetics and molecular genetics of childhood leukemia. *Hematol Oncol* 238
 1999;17:91–105. 239
- [2] Shu XO, Ross JA, Pendergrass TW, Reaman GH, Lampkin B, Robinson LL. Parental alcohol consumption, 240
 cigarette smoking, and risk of infant leukemia: a children's cancer group study. *J Natl Cancer Inst* 241
 1996;88:24–31. 242
- [3] Greaves MF, Chan LC, Furley AJ, Watt SM, Molgaard HV. Lineage promiscuity in hemopoietic differ- 243
 entiation and leukemia. *Blood* 1986;67:1–11. 244
- [4] Sawyers CL. Molecular genetics of acute leukemia. *Lancet* 1997;349:196–200. 245
- [5] Ching-Hon Pui, Williams EE, Pharn D. Acute lymphoblastic leukemia. *Drug Ther* 1998;339:605–13. 246
- [6] Nick G. Practical application of minimal residual disease assessment in childhood acute lymphoblastic 247
 leukemia. *Br J Haematol* 2001;112:275–81. 248
- [7] Diem M, Boydston-White S, Chiriboga L. Infrared spectroscopy of cells and tissues: shining light onto a 249
 novel subject. *Appl Spectrosc* 1999;53:148–61. 250
- [8] Ramesh J, Salman A, Argov S, Goldstein J, Sinelnikov I, Walfisch S, et al. FTIR microscopic studies on 251
 normal, polyp and malignant human colonic tissues. *Subsurf Sens Technol Appl* 2001;2:99–117. 252
- [9] Gao T, Feng J, Ci Y. Human breast carcinomas display distinctive FTIR spectra: implication for the 253
 histological characterization of carcinomas. *Anal Cell Pathol* 1999;18:87–93. 254
- [10] Schultz CP, Liu K, Johnston JB, Mantsch HH. Study of chronic lymphocytic leukemia cells by FT-IR 255
 spectroscopy and cluster analysis. *Leuk Res* 1996;20:649–55. 256
- [11] Ramesh J, Salman A, Hammody Z, Cohen B, Gopas J, Grossman N, et al. FTIR Microscopic studies on 257
 normal and H-Ras oncogene transfected cultured mouse fibroblasts. *Eur Biophys J* 2001;30(4):250–5. 258

- [12] Huleihel M, Salman A, Erukhimovitch V, Ramesh J, Hammody Z, Moredchai S. Novel optical method for study of viral carcinogenesis in vitro. *J Biochem Biophys Methods* (2001), in Press. 259
260
- [13] Salman A, Argov S, Ramesh J, Goldstein J, Igor S, Guterman H, et al. FTIR microscopic characterization of normal and malignant human colonic tissues. *Cell Mol Biol* 2001;47:OL159–66. 261
262
- [14] Hudson L, Poplack FC. *Practical immunology*. London: Blackwell; 1976. 263
- [15] Jackson M, Mantsch HH. Biomedical infrared spectroscopy. In: Mantsch HH, Chapman D, editors. *Infrared spectroscopy of biomolecules*. New York: Wiley-Liss; 1995. p. 311–40. 264
265
- [16] Benedetti E, Palatresi MP, Vergamini P, Papineschi F, Spemolla G. New possibilities of research in chronic lymphatic leukemia by means of Fourier transform-infrared spectroscopy II. *Leuk Res* 1985;9:1001–8. 266
267
- [17] Margolin JF, Poplack DG. Acute lymphoblastic leukemia. In: Philip AP, David GP, editors. *Principles and practice of pediatric oncology*. PA: Lippincott-Raven; 1997. p. 433–60. 268
269

UNCORRECTED PROOF